J Mater Sci: Mater Med (2011) 22:557–569
DOI 10.1007/s10856-011-4240-8

Ag-doped 45S5 Bioglass®-based bone scaffolds by molten salt ion exchange: processing and characterisation

P. J. Newby · R. El-Gendy · J. Kirkham · X. B. Yang · I. D. Thompson · A. R. Boccaccini

Received: 27 September 2010 / Accepted: 14 January 2011 / Published online: 4 February 2011

Abstract There is increasing interest in developing scaffolds with therapeutic and antibacterial potential for bone tissue engineering. Silver is a proven antibacterial agent which bacteria such as MRSA have little or no defense against. Using an ion exchange method, silver ions have been introduced into 45S5 Bioglass® based scaffolds that were fabricated using the foam replication technique. This technique allows the introduction of Ag^+ ions onto the surface of the scaffold without compromising the scaffold bioactivity and other physical properties such as porosity. Controlling the amount of Ag^+ ions introduced onto the surface of the scaffold was achieved by tailoring the ion exchange parameters to fabricate samples with repeatable and predictable Ag^+ ion release behavior. In vitro studies in simulated body fluid were carried out to ensure that the scaffolds maintained their bioactivity after the introduction of Ag^+ ions. It was also shown that the addition of low concentrations (2000:1 w/w) of silver ions supported the attachment and viability of human periodontal ligament stromal cells on the 3D scaffolds. This work has thus confirmed ion exchange as an effective technique to introduce Ag^+ ions into 45S5 Bioglass® scaffolds without compromising the basic properties of 45S5 Bioglass® which are required for applications in bone tissue engineering.

P. J. Newby · A. R. Boccaccini
Department of Materials, Imperial College London, Prince Consort Road, London SW7 2BP, United Kingdom

R. El-Gendy · J. Kirkham · X. B. Yang
Skeletal Tissue Engineering Laboratory, Leeds Dental Institute, University of Leeds, Leeds LS2 9L, United Kingdom

I. D. Thompson
Dental Biomaterials, King's College London, Guy's Hospital, London SE1 9RT, United Kingdom

A. R. Boccaccini (✉)
Institute of Biomaterials, Department of Materials Science and Engineering, University of Erlangen-Nuremberg, 91058 Erlangen, Germany
e-mail: aldo.boccaccini@ww.uni-erlangen.de

1 Introduction

Bioglass®-derived glass-ceramic scaffolds and related silicate systems have in recent years attracted increasing attention for bone tissue engineering (TE) strategies [1–3]. This is because they are suitable 3D porous matrices with the potential to promote new bone tissue formation, also providing mechanical support to the surrounding tissue; in essence they fulfil the basic requirements for an optimal material for use in bone TE [4]. These scaffolds not only exhibit highly interconnected porosity with suitable pore size, but they are also highly bioactive and osteoconductive. There are, however, still challenges remaining for the optimisation of the scaffolds before they can be rolled out for general use in a clinical setting related to achieving further functionalities for better in vivo performance.

With post-operative bacterial infections and implant rejection a concern [5], it is reasonable to postulate that for in vivo TE the ideal scaffold would be one that incorporates an antibacterial element to help to prevent infections and thus with the potential to reduce the post operative care and to improve the patient's recovery time. Therefore recent research in bone TE scaffolds is focussing on incorporating an antibacterial function [6–10].

The most common bacteria that cause these infections are *Staphylococcus aureus* and infections can normally be treated with antibiotics such as gentamicin and vancomycin

[11, 12]. However a growing problem is that bacteria may have become resistant to antibiotics because they have been over used to combat infections [12]. These are called methicillin-resistant *S. aureus* strains (MRSA) and vancomycin-resistant *S. aureus* (VRSA), with MRSA being the most common [13]. With these resistance strains of bacteria causing increasing problems in healthcare, alternative solutions need to be found not only regarding orthopaedic implants but also for TE approaches.

Silver has long been a known antibacterial element [8, 14, 15] and it has been proposed for the treatment of bone infections. The anti-bacterial effect of the silver ion has been attributed to the very small size and therefore high surface to volume ratio [14]. This allows the metal ions to interact closely with the membranes of the bacteria. This close interaction causes the silver ions to be incorporated into the bacteria cell membrane and this causes the intercellular substances to leak out of the cell leading to cells death [14]. Silver ions also have a negative effect on the bacteria's ability to colonize, which will control the spread of infection around an implant. The concentration of silver used needs to be carefully controlled as high levels of silver will cause cell cytotoxicity. This toxic effect also occurs at a high release rate of silver ions, so when incorporating silver into biomaterials for orthopaedic or TE applications this effect needs to be taken into consideration [7, 8].

There are several ways of introducing metal ions into a silicate scaffold, including the traditional melt quenching technique, sol–gel processing and molten salt ion-exchange methods. Work has already been done on introducing silver into silicate [16–18] and phosphate based glass-ceramics [19] through the sol–gel technique. Sol–gel methods are useful if silver is required throughout the whole structure of the scaffold [17], however the preferred approach is that the silver ion should act as an initial potent antibacterial agent whilst the risk of infection is at its highest. This approach requires that silver ions are only present on the surface of the scaffold and an obvious processing choice to incorporate the ion in the outer surface layer of the 3D scaffold is therefore the molten salt ion-exchange technique [8].

Molten salt ion exchange is a well known method which has been investigated for the last few decades for introducing ions into silicate glass, for example for waveguides for optical applications [20]. Di Nunzio et al. [8] were the first to show that by using molten salt ion exchange silver ions can be introduced into bioactive silicate glasses. This method allows the fabrication of samples that can be easily reproduced, with constant diffusion profiles and silver content, offering a simple and low cost way to introduce silver into a glass-ceramic after it has been sintered to its final required shape and dimensions [8]. The glass-ceramic used by Di Nunzio et al. [8] had a composition in the system SiO_2-CaO-Na_2O and silver was introduced by exchanging the sodium ions in the glass with silver ions in the molten salt. "It should be noted that the preliminary study of Di Nunzio et al. [8] was carried out using solid glass-ceramic pellets although for tissue engineering applications current work should consider highly porous glass-ceramic scaffolds". The ion exchange mechanism is represented by the following equilibrium equation: [8]

$$Na^{+}_{(glass)} + Ag^{+}_{(melt)} \xrightarrow{heat} Ag^{+}_{(glass)} + Na^{+}_{(melt)}.$$

The molten salt bath contained silver nitrate and sodium nitrate salts, with the sodium nitrate salt used to regulate the amount of silver being exchanged into the material; this exchange process is described by the following reaction:

$$Na_2O + 2AgNO_2 \xrightarrow{heat} 2NaNO_3 + Ag_2O.$$

45S5 Bioglass®-derived glass-ceramic scaffolds with a composition in the SiO_2-Na_2O-CaO-P_2O_5 system, which have been developed and characterised in previous studies [1, 21] could undergo a similar ion exchange process, as the glass-ceramic pellets described by Di Nunzio et al. [8]. In the present research the ion exchange technique was adapted to incorporate Ag ions into Bioglass®-derived glass-ceramic 3D scaffolds. The bioactivity and cell response of the scaffolds incorporating silver ions were investigated for the first time using human periodontal ligament stromal cells. The aim was to assess whether or not the incorporation of Ag would have an effect on the well established bioactivity and cellular response of Bioglass® based scaffolds.

2 Materials and experimental procedure

2.1 Scaffold fabrication

The bioactive glass-ceramic scaffolds used in this work were produced using the foam replication technique developed by Chen et al. [1]. This technique has been discussed in detail in the previous work so only specific parameters used in the present research will be indicated here. The starting bioactive glass powder selected for this work was 45S5 Bioglass® with the standard composition of 45wt% SiO_2, 24.5wt% Na_2O, 24.5wt% CaO and 6wt% P_2O_5. The 45S5 Bioglass® has a density of 2.70 g cm^{-3} with a particle size in the range 10–20 μm. Polyurethane (PU) foam (Reticel, Corby, UK) was used as the sacrificial template in the foam replica method and polyvinyl alcohol (PVA) (Sigma–Aldrich, UK) was used as the binder. The PU foam has 45 pores per inch (ppi) and was cut into 20 × 20 × 10 mm^3 blocks in anticipation that during the

sintering process the green bodies would shrink by approximately 50% [1]. The green bodies were sintered at 1,100°C with a pre-sintering step which burnt off the binder and the sacrificial PU foam at 550°C.

2.2 Silver ion exchange

The pre-fabricated 45S5 Bioglass® scaffolds were modified using ion exchange following a similar procedure as the one described by Di Nunzio et al. [8]. The scaffolds and the salt bath of silver nitrate ($AgNO_3$) and sodium nitrate ($NaNO_3$), obtained from VWR and Sigma–Aldrich, UK, respectively, in a ceramic crucible, were placed in a furnace at 400°C. This temperature was selected as it is above the melting points of both nitrate salts (210°C and 310°C, respectively) and will ensure that the salt bath is molten. The scaffolds where then dipped into the molten salt bath for 30 min. The scaffolds were then manually removed and allowed to cool down on a ceramic plate at room temperature. Once cooled, the scaffolds were then washed in distilled water to remove any residue traces of the nitrate salts from the ion exchange process.

The following study was split into three parts with the preliminary tests investigating whether or not the technique described by Di Nunzio et al. [8] could be applied not only to the 45S5 Bioglass® derived glass-ceramic but to porous scaffolds instead of pellets. The second part of the experiments was aimed at optimising the ion exchange process for the present scaffolds including also the characterisation of the newly formed silver ion impregnated scaffolds, investigating bioactivity and mechanical properties. Finally selected Ag containing scaffolds were investigated in terms of their cell biology response.

2.2.1 *Preliminary silver ion exchange study*

This study used the concentrations of $AgNO_3$ and $NaNO_3$ that were described originally by Di Nunzio et al. [8] and are shown in Table 1. The objective was to apply for the first time the same technique described in that work to 45S5 Bioglass®-derived scaffolds. To ascertain if the technique was successful a number of characterisation tests were carried out.

X-ray diffraction (XRD) analyses were conducted using a Phillips PW 1700 series instrument using Cu Kα incident radiation with the resulting spectra being analysed using X'Pert high Score software and the PCPDF data base to obtain the crystalline composition of the scaffolds [22]. The microstructure of the scaffolds was observed using a variable pressure JEOL JSM 5610LV scanning electron microscope (SEM). The intention was to compare the silver ion exchange scaffolds (labelled AgIE scaffolds) microstructure with that of the original 45S5 Bioglass® scaffolds, in order to investigate a possible microstructural effect of the ion exchange process. Energy dispersive X-ray spectroscopy (EDX) was used to determine the elemental composition of the struts. Using these characterisation tests the viability of the ion exchange technique was evaluated. Moreover, it was also investigated how the ion exchange method could be improved and optimised (next section).

2.2.2 *Main silver ion exchange study*

From the results and general observations made throughout the preliminary study described above the following changes were made to the original ion exchange procedure:

- Introduction of a controlled rate of heating and cooling during the ion exchange process to help prevent thermal shock fracture of the scaffolds that was seen to occur previously. The scaffolds and the salt bath were heated up to 400°C at a rate of 2°C per minute and cooled down at a rate of 2°C per minute.
- Concentrations of $AgNO_3$ and $NaNO_3$ were altered to more appropriate concentrations based on the results and observations from the preliminary study (shown in the Sec 3, see below) and the observations made by Di Nunzio et al. [8]. The new concentrations are shown in Table 1. The two new concentrations fall between the original medium and low concentrations.

Table 1 Concentrations and quantities of sodium nitrate and silver nitrate used for the silver molten salt ion exchange experiments, according to Di Nunzio et al. [8] and new values determined for this study

Sample name	Description of sample	Ratio of sodium nitrate to silver nitrate	Mass of sodium nitrate (g)	Mass of silver nitrate (ml)
PreHigh	Preliminary high	20 to 1	4.25	50
PreMed	Preliminary medium	200 to 1	42.5	50
Prelow	Preliminary low	2,000 to 1	42.5	5
High	High concentration of silver	800 to 1	42.5	12.5
Med	Medium concentration of silver	1,400 to 1	42.5	7.14
Low	Low concentration of silver	2,000 to 1	42.5	5

- Increased washing time after the ion exchange process, this was necessary due to the observation of an excess amount of salt residue on the surface of the scaffold.
- The immersion time was varied for optimisation purposes and immersion periods of 15, 30, 45 and 60 min were investigated.

2.3 Material characterisation

The characterisation techniques used in the preliminary study described above (XRD, SEM/EDX) were repeated and additional tests were carried out to fully characterise the new scaffolds.

Fourier transform infra-red spectroscopy (FTIR) was used to identify specific chemical bonds in the scaffolds using a Bruker Vector 22 TGA-IR instrument and a transmission spectra attachment. The scaffolds were ground into powder and combined with potassium bromide (KBr, Sigma–Aldrich, UK) and pressed into pellets with a diameter of 13 mm.

The acellular in vitro bioactivity of the scaffolds was assessed by soaking them in simulated body fluid (SBF) for 1, 3, 7, 11 and 15 days and then analysed using XRD, SEM, EDX and FTIR to determine the possible precipitation of hydroxyapatite (HA) on the scaffold surfaces. The SBF was prepared according to the standard procedure suggested by Kokubo et al. [23]. Formation of HA on biomaterial surfaces in contact with SBF is usually considered the first marker to assess the bioactive behaviour of biomaterials intended for applications as bone replacement materials and in bone regeneration [24]. As porosity is an important property of scaffolds [4] it needs to be measured carefully to ensure that it is not being significantly altered by the ion exchange process. This measurement also gives an indication of how much residue salt may have been left on the surface of the scaffold. The porosity of a scaffold can be calculated using the following equation:

$$\text{Porosity} = 1 - \left(\frac{\rho_{\text{scaffold}}}{\rho_{\text{material}}}\right) = 1 - \left(\frac{m_{\text{scaffold}}}{\upsilon_{\text{scaffold}} \times \rho_{\text{material}}}\right), \quad (1)$$

where ρ_{scaffold} and ρ_{material} are the densities of the scaffold and of Bioglass®, respectively, m_{scaffold} is the mass of the scaffold and v_{scaffold} is the total volume of the scaffold.

The compressive strength of the scaffolds was evaluated using a Zwick testing machine on $10 \times 5 \times 5$ mm^3 prismatic samples. This analysis was carried out for all concentrations and for all salt bath immersion periods and after 14 days SBF immersion to give complete information about the possible effect of the introduction of silver ions on the scaffolds compressive strength.

2.4 Cell culture studies

Human periodontal ligament stromal cells (HPDLCs) were isolated as described by Somerman et al. [25], from explants scraped off the mid root surface of freshly extracted premolar/wisdom teeth. The teeth were obtained with patients' consent as donations to the Leeds Dental Institute (LDI) Research Tissue Bank (LREC 07/H1306/93). Cells outgrowing from human periodontal ligament explants were cultured in monolayers on tissue culture plastic in alpha modified minimum essential medium (α-MEM, Lonza) supplemented with 20% foetal bovine serum (FBS, Lonza), 2 mM of L-glutamine (Sigma) and 100 units/ml penicillin/streptomycin (Gibco). The cells were incubated at 37°C under 5% CO_2 and the media changed weekly until the cells had reached 90% confluence. The scaffold samples were cut to $2 \times 2 \times 2$ mm^3 and sterilised using UV irradiation; 2×10^5 cells (passage 4) were dynamically seeded either onto plain 45S5 Bioglass® scaffolds (controls) or onto each of three of the silver ion exchanged Bioglass® scaffolds (low, medium and high samples as defined in Table 1) and maintained in the dynamic seeding apparatus for 3 days at 37°C, 5% CO_2. The cell–scaffold constructs were then cultured statically in tissue culture plates for a further 7 days and cell attachment and viability on the scaffolds confirmed by staining with live/dead fluorescent markers using CellTrack™ Green CMFDA (5-chloromethylfluorescein diacetate). Non-viable cells were stained using ethidium homodimer-1. The stained constructs were then viewed by confocal laser scanning microscopy (CLSM).

3 Results and discussion

3.1 Preliminary Ag^+ ion exchange study

The porosity of the present scaffolds was confirmed as ranging from 90% up to 95%, calculated using Eq. 1. This range of values is in agreement with results found in previous work for scaffolds fabricated by the foam replica method [1]. The highly porous structure can be seen in Fig. 1a and this confirms that highly porous 45S5 Bioglass® scaffolds with suitable pore architecture similar to spongy bone have been produced. The scaffolds produced here are similar to those described by Chen et al. [21], indicating the reliability of the foam replication technique as a robust and reproducible manufacturing method for bone tissue scaffolds. From the SEM image (Fig. 1b) small crystalline grains are observed, with diameters of approximately 0.5 μm, which indicates that the scaffold is partially crystallised. The preliminary study was carried out using the three concentrations originally proposed by Di

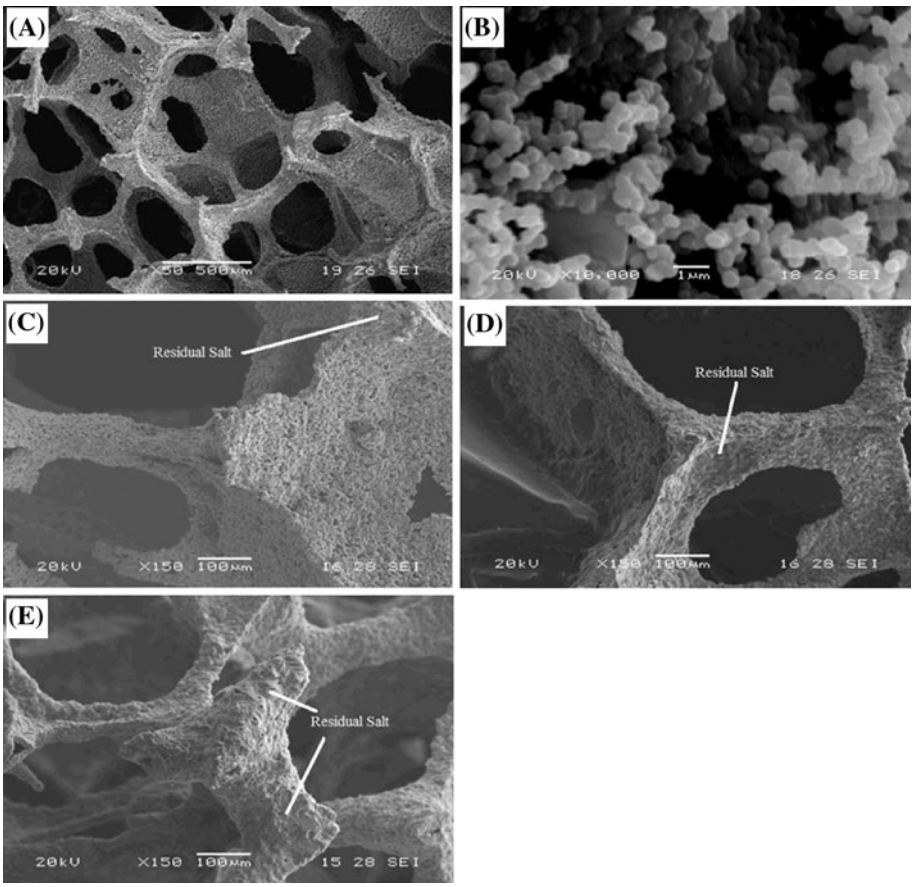

Fig. 1 SEM images of Bioglass®-derived scaffolds investigated: **a** plain 45S5 Bioglass® scaffold at a low magnification, **b** plain 45S5 Bioglass scaffold at a high magnification, **c** preliminary low concentration Ag^{+}/45S5 Bioglass® scaffold, **d** preliminary medium concentration Ag^{+}/45S5 Bioglass® scaffold and **e** preliminary high concentration Ag^{+}/45S5 Bioglass® scaffold

Nunzio et al. [8], as shown in Table 1. Figure 1 shows that whilst the porosity and the structure of the scaffolds have been maintained there is residual salt found on the surface of the scaffold (Fig. 1c–e), indicating that the scaffolds require a more rigorous washing process to solve this issue after the ion exchange process and that this should be addressed in the optimisation phase.

EDX analysis results on treated (ion exchange) and non-treated scaffolds are shown in Fig. 2. They show the presence of silicon, sodium, calcium and gold, the presence of gold is due to the coating applied for SEM observations (Fig. 2a). The EDX analysis on ion exchanged specimens also indicates the presence of silver, confirming that the ion exchange method has been successful (Fig. 2b). However, it was also evident that levels of silver present in the sample which was immersed in the lowest concentration salt bath were not detected. This could be because the concentration of silver was lower than the detection limit of EDX analysis. Despite taking EDX data at various points across the sample, the concentration of silver was seen to be extremely low. The EDX data thus suggest that the ion exchange technique is appropriate when the correct salt bath concentration is used and the concentration of Ag in the scaffold depends on the concentration of the salt bath.

The crystalline nature of the samples was confirmed by XRD analysis as shown in Fig. 3, with Fig. 3a showing the XRD pattern of the partially crystallised structure of the (as fabricated) 45S5 Bioglass® scaffolds. It is shown that the spectrum matches that of the crystalline phase $Na_6Ca_3Si_4O_{18}$, which is in agreement with previous results [1]. Comparing the results in Fig. 3a to those in Fig. 3b–d, it can be observed that $Na_6Ca_3Si_6O_{18}$ is still present in all samples after ion exchange. Figure 3d shows the presence of silver (Ag and Ag_3PO_4 peaks). The presence of Ag_3PO_4 is repeated in the low and medium concentration XRD spectra (Fig. 3b and c), however these two spectra are lacking the presence of the pure Ag peaks. Thus XRD analyses provide further confirmation about the presence of silver in the structure of the Bioglass® based scaffolds. Since XRD analysis detected silver peaks in the lowest concentration samples, it can be conclusively stated that the molten salt ion exchange was successful even at such low silver concentrations of the starting salt bath.

Di Nunzio et al. [8] have stated that the best salt concentration out of the three investigated was the lowest as this concentration still imparted the Ag ions into the glass-ceramic structure whilst not having a detrimental effect on the HA formation (bioactivity study, see below) on the

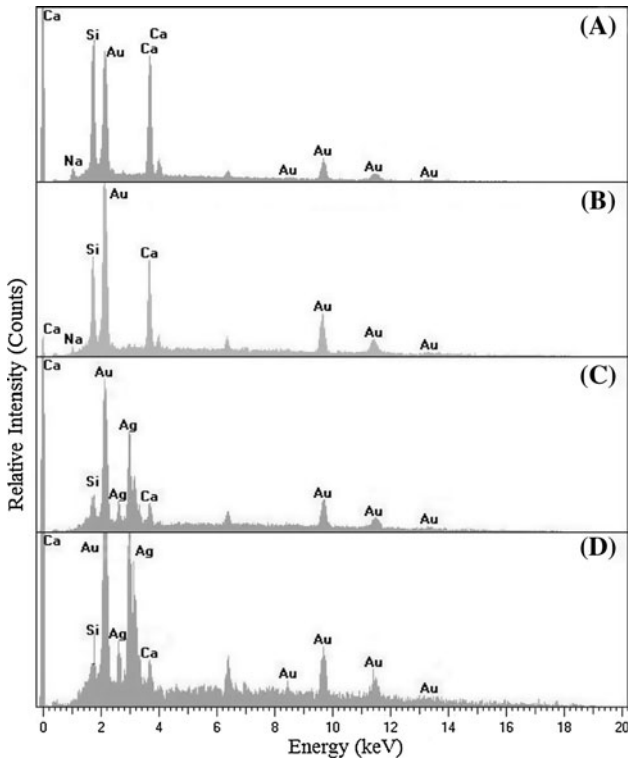

Fig. 2 EDX analysis on scaffolds for the preliminary concentrations of silver used in the ion exchange process: **a** plain 45S5 Bioglass®-derived scaffold, **b** preliminary low concentration Ag^+/45S5 Bioglass® scaffold, **c** preliminary medium concentration Ag^+/45S5 Bioglass® scaffold and **d** preliminary high concentration Ag^+/45S5 Bioglass® scaffold

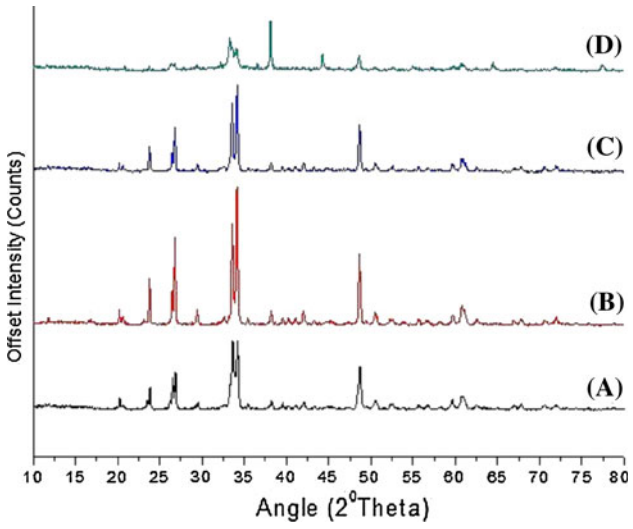

Fig. 3 XRD analysis of scaffolds for the preliminary concentrations of silver used in the ion exchange process: **a** plain 45S5 Bioglass® scaffold, **b** preliminary low concentration Ag^+/45S5 Bioglass® scaffold, **c** preliminary medium concentration Ag^+/45S5 Bioglass® scaffold and **d** preliminary high concentration Ag^+/45S5 Bioglass® scaffold

material and not inducing a toxic effect on cells. In a full optimisation study, the immersion period of the sample in the molten salt bath needs to be taken into account too. As in Di Nunzio et al. [8] study, in the present investigation the lowest salt bath concentration was successful to incorporate silver into the silicate (Bioglass®) network and it was therefore proposed that a new set of relatively low concentrations be scrutinised, these are listed in Table 1. In our optimisation study, these concentrations were selected between the preliminary studied lowest and medium concentrations, as discussed in the next section.

3.2 Main Ag^+ ion exchange study

The respective SEM analyses of all samples investigated in the optimisation study are shown in Fig. 4a–d. The analysis of samples from all concentrations and all immersion periods showed that the salt residue present, which was considerable (e.g. in Fig. 1c–e), has been vastly reduced but it is still present, demonstrated in Fig. 4b–d whilst maintaining the general structure and porosity of the plain 45S5 Bioglass® scaffolds (Fig. 4a).

The porosity study carried out on these scaffolds is shown in Fig. 5. As indicated above, the plain 45S5 Bioglass® scaffolds have a porosity of above 90% and this is in accordance with the literature [1]. On the other hand, unwashed scaffolds after the ion exchange process have porosity in the range of 37–75% and the scaffolds that have been washed in distilled water after the ion exchange process have porosity in the range of 65–85%. Figure 5 shows that scaffolds treated using the lowest salt concentration exhibit porosity varying in a wider range than that of scaffolds treated using higher concentration salt baths. It can also be seen that as the immersion period increases the porosity range decreases. The decrease in porosity of the scaffolds is mainly due to the presence of the solidified salt melt residue on the surface of the struts. It should be noted that whilst the salt melt is soluble in distilled water so is the 45S5 Bioglass® based scaffold. This means that leaving the ion exchanged scaffold for an extended period in distilled water would probably have a detrimental effect on the scaffold mechanical properties. Since both silver nitrate and sodium nitrate are also soluble in alcohol, specifically ethanol, work should be done to assess if a washing process in an alcohol could reduce the salt residue without compromising the mechanical properties. It can be theorised that the lowest salt concentration scaffolds exhibit a wider porosity range due to the lower silver nitrate content in the salt melt; porosity range generally decreases with increasing silver nitrate content. The mechanism behind this behaviour is not known as of yet. It was observed that scaffolds which had been immersed for longer periods of time had formed layers of the salt residue on the scaffold

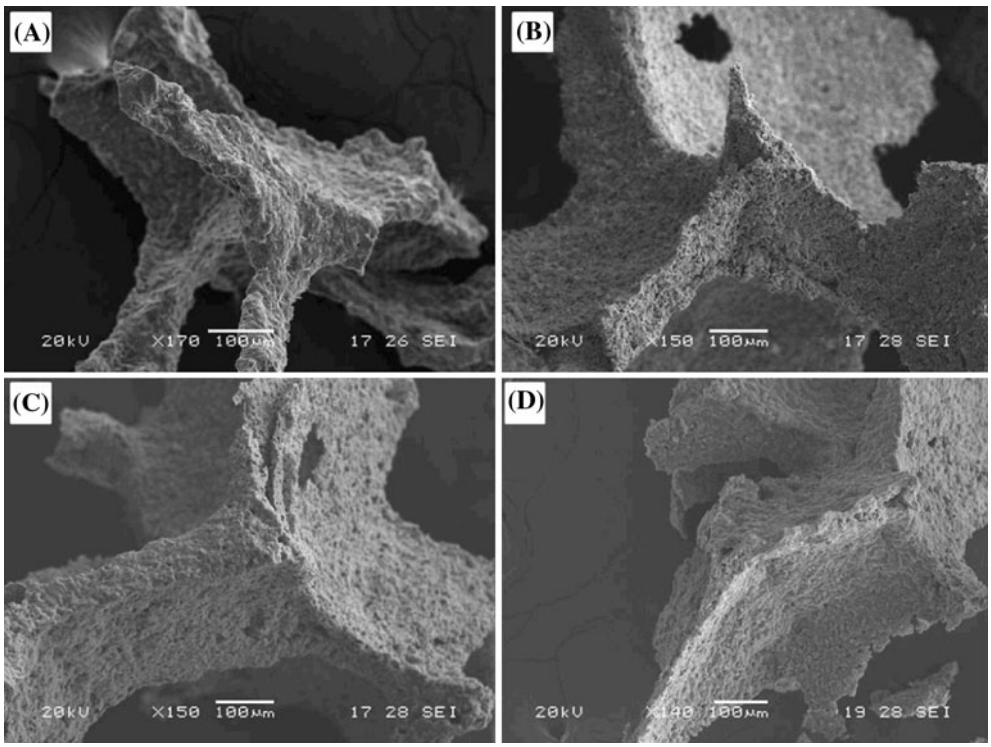

Fig. 4 SEM images of scaffolds treated by ion exchange for 30 min at different concentrations: **a** plain 45S5 Bioglass® scaffold, **b** low concentration Ag^{+}/45S5 Bioglass® scaffold, **c** medium concentration Ag^{+}/45S5 Bioglass® scaffold and **d** high concentration Ag^{+}/45S5 Bioglass® scaffold

and that these long immersion scaffolds were easier to clean as the layers had a tendency to detach leaving the scaffold almost untouched underneath them.

The results of the EDX analysis on these scaffolds are presented in Fig. 6a–d. Similar results to those shown in Fig. 2 with the presence of silicon, sodium, calcium and gold in all four spectra are obtained. Silver was detected in the medium and higher concentration samples (Fig. 6c and d), for all immersion periods, however, the presence of silver was not detected in the lower concentration samples at the shorter immersion periods, similar to the previous results shown in Fig. 2b. However, longer immersion periods at the lowest concentration of silver did yield EDX spectra showing silver peaks, indicating that a long enough immersion period is required for the successful incorporation of silver at the lowest Ag concentrations. The detection threshold of the

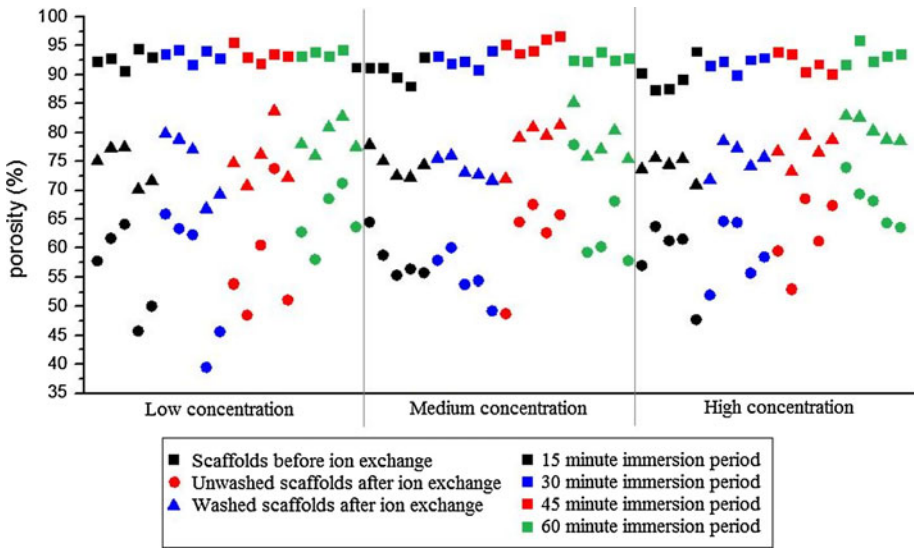

Fig. 5 Porosity study graph showing porosities for all three concentrations over all four immersion periods

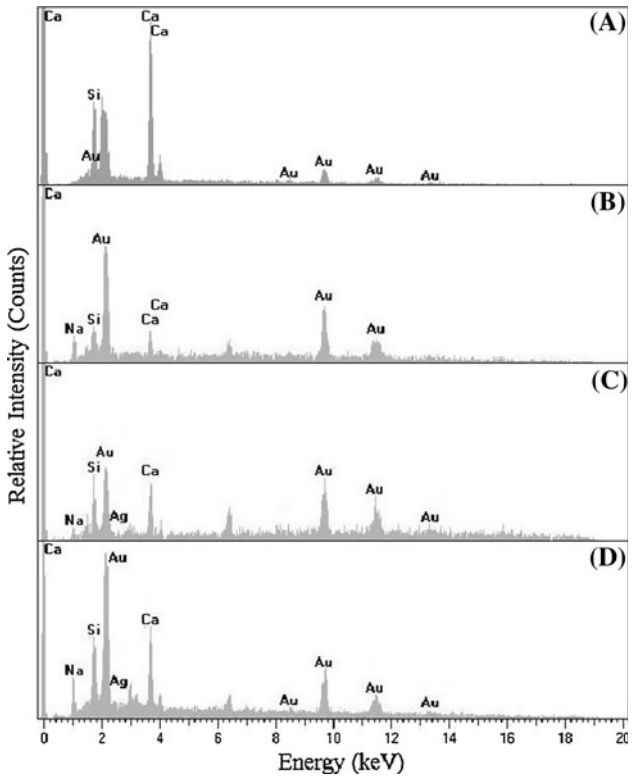

Fig. 6 EDX analysis on scaffold surfaces for the main concentrations of silver after immersion in the salt bath for 15 min: **a** plain 45S5 Bioglass® scaffold, **b** low concentration Ag^+/45S5 Bioglass® scaffold, **c** medium concentration Ag^+/45S5 Bioglass® scaffold and **d** high concentration Ag^+/45S5 Bioglass® scaffold

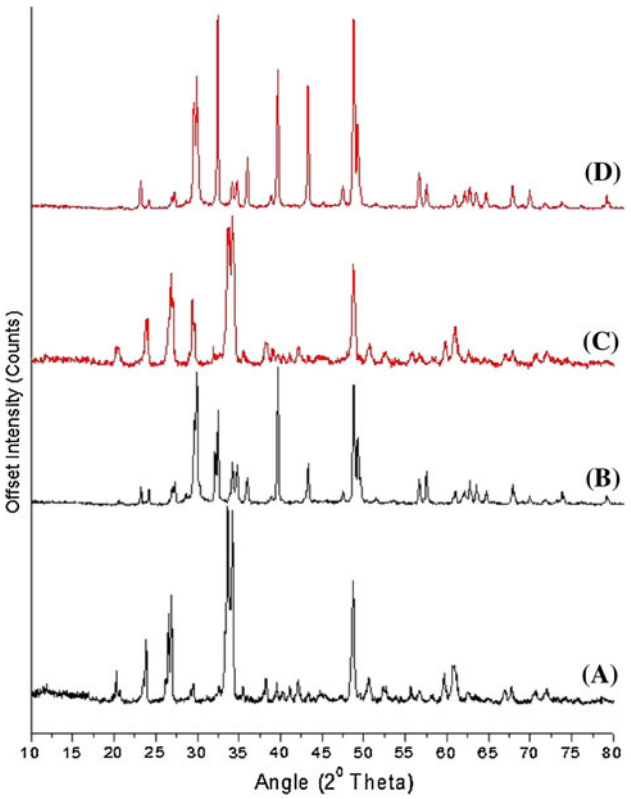

Fig. 7 XRD analysis on scaffold surfaces for the main concentrations of silver after an immersion period of 15 min in the salt bath: **a** plain 45S5 Bioglass® scaffold, **b** low concentration Ag^+/45S5 Bioglass® scaffold, **c** medium concentration Ag^+/45S5 Bioglass® scaffold and **d** high concentration Ag^+/45S5 Bioglass® scaffold

instrument, however, should be considered, and it is highly likely that scaffolds ion exchanged in the lowest Ag concentration bath for low immersion times have incorporated Ag at a level below the detection limit of EDX analysis.

XRD results are shown in Fig. 7. Peaks corresponding to $Na_6Ca_3Si_6O_{18}$ can be seen in all four spectra in Fig. 7a–d as well as the rest of the samples, which is in accordance with previous work [1]. Figure 7b–d shows the presence of pure silver with a peak at approximately $2\theta = 30$ degrees, while Fig. 7b and d show the presence of Ag_3PO_4 peaks between $2\theta = 37$ and $2\theta = 48$ degrees. These results agree with the preliminary study and are also repeated through the other investigated samples treated at different immersion times. XRD analysis confirmed also the presence of silver in the lower concentration samples.

FTIR analyses were carried out on scaffolds and the results are shown in Fig. 8. The aim was to characterise the chemical composition of the scaffold's surface considering that FTIR has not been used to characterise the present scaffolds before. FTIR results show that the dual Si–O peaks fall in the region 1,097–1,100 cm^{-1} and 1,037–1,050 cm^{-1}. Moreover there is a non-bridging oxygen peak lying between 920 and 940 cm^{-1}, dual P–O peaks between 720–650 cm^{-1} and 625–580 cm^{-1} and finally a dual Si–O peak appears between 528–536 cm^{-1} and 455–457 cm^{-1}, as shown in Fig. 8a. These bond peaks are consistent with results in the literature [26]. The spectra shown in Fig. 8b–d indicate the presence of the dual P–O peaks at 720–680 cm^{-1} and at 625–580 cm^{-1}. The spectra have also the Si–O peak at 528–536 cm^{-1}. All of these peaks have been shown to occur in plain 45S5 Bioglass® [26, 27]. The peak at 1,387 cm^{-1} is from NO_3^- which will have originated from the salt, $AgNO_3$ [28]. The peaks at 950–1,000 cm^{-1} and 670–680 cm^{-1} are due to the Si–O–Ag bond and this is shown in all four spectra, which indicates that the silver has been incorporated in the structure of the 45S5 Bioglass®-derived glass-ceramic scaffolds [16, 28].

3.3 Bioactivity tests in SBF

Figure 9 shows SEM images after the scaffolds have been immersed in SBF for 15 days. The presence of HA on the surface of the scaffold after 15 days of immersion in SBF on both the plain 45S5 Bioglass® scaffolds and the Ag^+/45S5 Bioglass® scaffolds is clearly identified. This result confirms that the presence of silver in the scaffold surface

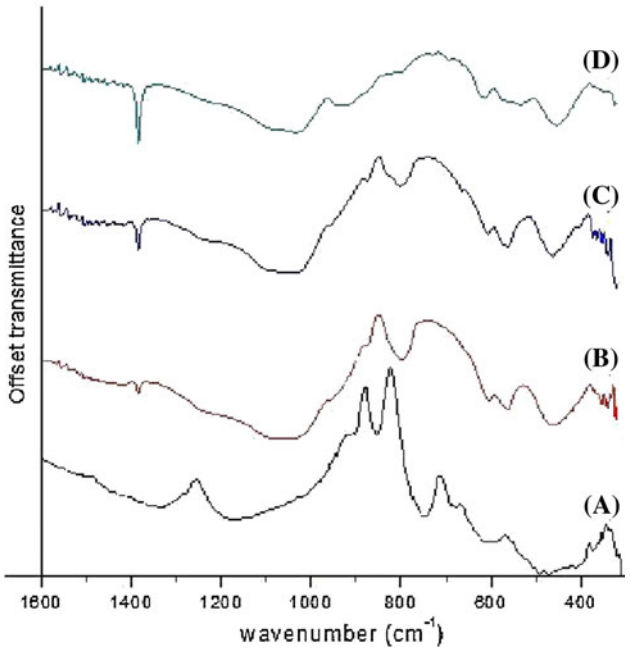

Fig. 8 FTIR analysis on scaffold surfaces for the main concentrations of silver after 60 min period of immersion in the salt bath: **a** plain 45S5 Bioglass® scaffold, **b** low concentration Ag^{+}/45S5 Bioglass® scaffold, **c** medium concentration Ag^{+}/45S5 Bioglass® scaffold and **d** high concentration Ag^{+}/45S5 Bioglass® scaffold

does not affect the formation of HA on the surfaces in contact with the SBF. HA formation on bioactive glass surfaces in contact with SBF is a well documented process [24] and is considered the marker for the bioactivity of a material intended for bone TE [1]. The process of HA formation can be described in several stages starting with the exchange of sodium within the silicate glass-ceramic with H^{+} or H_3O^{+} from the solution [29]. The next stage involves the loss of soluble SiO_2 (in the form of $Si(OH)_4$) to the surrounding solution. This results in the formation of Si–OH on the surface of the glass-ceramic after the Si–O–Si bonds break [29]. Subsequently, condensation and re-polymerisation of a SiO_2-rich layer on the surface of the scaffold occurs. The next process involves Ca^{2+} and $PO_4{}^{3-}$ groups migrating to the surface through the SiO_2-rich top layer. These groups then form a $CaO\text{-}P_2O_5$-rich film on top of the SiO_2-rich layer. The new $CaO\text{-}P_2O_5$-rich film grows further by incorporating phosphate and calcium ions from the SBF medium. Lastly the amorphous $CaO\text{-}P_2O_5$ film crystallizes through the incorporation of OH^{-}, $CO_3{}^{2-}$, or F^{-} anions [24, 29].

The compressive strength of the scaffolds is affected by the ion exchange process, compressive strength values for all three concentrations over the four immersion periods before and after immersion in SBF are shown in Table 2. The results indicate that the ion exchange process increases the compressive strength of the scaffolds with differences between the concentrations, immersion periods and pre and post SBF immersion processes. The compressive strength increases with both the concentration and the immersion period with the highest compressive strength being 0.73 ± 0.04 MPa for the highest concentration after 60 min. The compressive strength decreased after the immersion in SBF but the values for the three concentrations where still higher than the value for the plain scaffold after 14 days in SBF. The difference between the immersion periods after immersion in SBF has decreased compared to before the samples were exposed to SBF, this could be due to the fact that SBF removes excess salt residues from the scaffolds resulting in all samples behaving similarly after a certain immersion period. In Bioglass®, the silicate network containing calcium and sodium as network modifiers incorporates the phosphate in the form of orthophosphate which is charge balanced by the calcium network modifier [30]. When silver ions exchange with sodium ions, which are ionically bonded to a non-bridging oxygen, they also interact with nearby bridging oxygens to form a two-coordinate structure [30]. This extra interaction is caused because silver ions can lose their outer electron more easily than sodium ions. This extra bond formed could affect the mechanical strength marginally. EDX results on samples after immersion in SBF are shown in Fig. 10. Increased levels of Ca and P ions in the scaffolds' structure can be inferred from the data in Fig. 10 compared with the levels shown in Fig. 6, which shows Ca and P levels before SBF immersion, and this is a clear indication of the bioactivity of the scaffold, which is also in broad agreement with previous results [1]. The presence of HA on the scaffolds surface after 15 days in SBF, which can be inferred from the Ca/P ratio in the EDX patterns, confirms that 45S5 Bioglass®-based scaffolds are suitable for bone TE as they are highly bioactive and that the presence of silver has not affected the bioactivity.

The immersion of the scaffold in SBF has an effect on the FTIR spectra as shown in Fig. 11. The main peaks that indicate the presence of HA are the dual P–O bonds at 625–580 cm^{-1} and 720–650 cm^{-1}; these peaks will grow in size as the length of time in SBF increases. The Si–O peak at 455–457 cm^{-1}, on the other hand, decreases over the immersion period of the scaffold in SBF. These two facts are indicative of HA formation on the surface of the scaffold and are shown in Fig. 11a [26, 27]. All three spectra of silver containing scaffolds shown in Fig. 11 confirm the indicators of HA formation. In particular, the P–O bonds at 600–604 cm^{-1} and 550–525 cm^{-1} in Fig. 11 are seen to increase with increased immersion time in SBF. In Fig. 12b the Si–O peak at 455–457 cm^{-1} is seen to decrease with increased immersion time in SBF and the Si–O peaks at 1,097–1,100 cm^{-1} and 1,037–1,050 cm^{-1} have flattened out [27]. The non-bridging oxygen peak lying

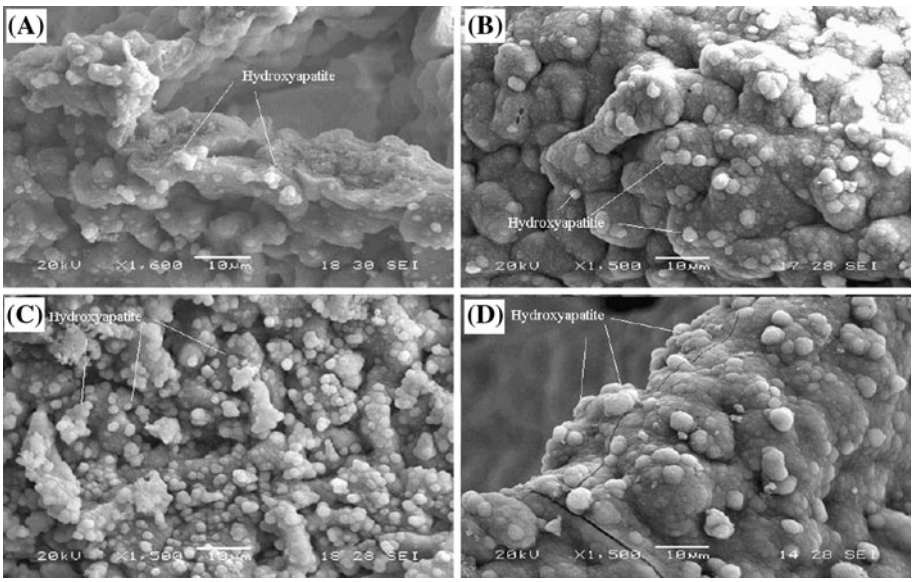

Fig. 9 SEM images of scaffold struts after a immersion period of 15 min in salt bath and after immersion in SBF for 15 days: **a** plain 45S5 Bioglass® scaffold, **b** low concentration Ag^{+}/45S5 Bioglass® scaffold, **c** medium concentration Ag^{+}/45S5 Bioglass® scaffold and **d** high concentration Ag^{+}/45S5 Bioglass® scaffold

Table 2 Compressive strengths of plain and ion exchanged scaffolds covering all three concentrations over the four immersion periods

Immersion period	Compressive strength in MPa		
	Low concentration	Medium concentration	High concentration
Before immersion in SBF			
15	0.62 ± 0.04	0.65 ± 0.07	0.68 ± 0.06
30	0.64 ± 0.03	0.66 ± 0.07	0.69 ± 0.09
45	0.65 ± 0.06	0.68 ± 0.04	0.72 ± 0.05
60	0.67 ± 0.06	0.70 ± 0.08	0.73 ± 0.04
Plain scaffold	0.53 ± 0.08		
After 14 days in SBF			
15	0.50 ± 0.04	0.51 ± 0.06	0.55 ± 0.05
30	0.50 ± 0.5	0.53 ± 0.05	0.56 ± 0.04
45	0.51 ± 0.06	0.52 ± 0.06	0.55 ± 0.06
60	0.49 ± 0.03	0.53 ± 0.08	0.58 ± 0.07
Plain scaffold	0.43 ± 0.05		

between 920 and 940 cm^{-1} is still present in Fig. 11b–d, but it is seen to have shrunk compared to Fig. 8, indicating that the non-bridging oxygen's are becoming bridging oxygen's by forming P–O bonds. It should be noted that if the Si–O peak at 455–457 cm^{-1} is still large, it could indicate that the HA layer is very thin or discontinuous [26, 27].

3.4 Cell viability on Ag substituted scaffolds

Figure 12 shows that all silver substituted scaffolds as well as the controls (non-substituted scaffolds) exhibited green fluorescent viable cells attaching to the scaffolds. No dead cells were apparent. However, the highest number of cells attached to the scaffolds was seen in those constructs with the lowest concentration of silver and in the control scaffolds. In general, the presence of Ag^{+} ions at low concentrations appeared to have supported cell attachment and maintained cell viability on the scaffolds up to 7 days in vitro. However, scaffolds containing higher concentrations of Ag^{+} appeared to have reduced cell attachment. This preliminary data illustrates that a low silver ion concentration in Bioglass®-derived glass-ceramic scaffolds has no obvious detrimental effects on cell attachment and viability compared to the control 45S5 Bioglass® scaffolds without silver.

These results coincide with the recent report by Xing et al. [31] who used poly-3 hydroxy butyricacid-*co*-3-hydroxy valeric acid nanofibers loaded with 5–13 nm silver particles and showed that there were no signs of cytotoxicity on NIH3T3 fibroblast cells [31]. However, Balagna et al. [9] showed recently that Ag-bioactive glass scaffolds inhibited MG63 osteoblast cell proliferation and differentiation after 4 days of culture compared to the control

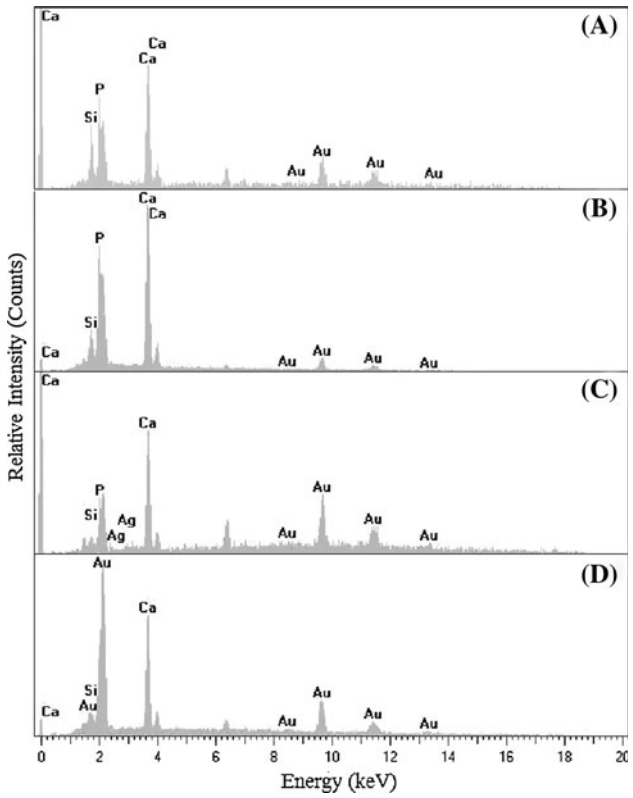

Fig. 10 EDX analysis of scaffold for the main concentrations of silver after immersion in salt bath for 15 min and after immersion in SBF for 15 days: **a** plain 45S5 Bioglass® scaffold, **b** low concentration Ag^+/45S5 Bioglass® scaffold, **c** medium concentration Ag^+/45S5 Bioglass® scaffold and **d** high concentration Ag^+/45S5 Bioglass® scaffold

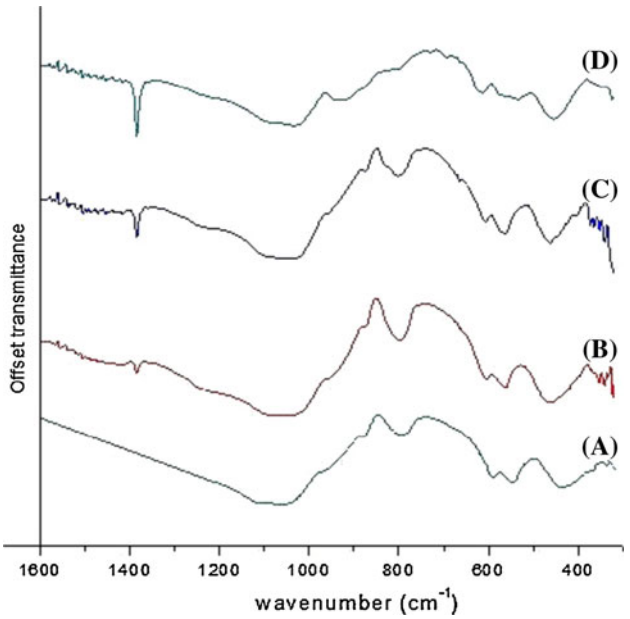

Fig. 11 FTIR analysis on scaffolds for the main concentrations of silver after the scaffolds were immersed in the salt bath for 30 min and after immersion in SBF for 15 days: **a** plain 45S5 Bioglass® scaffold, **b** low concentration Ag^+/45S5 Bioglass® scaffold, **c** medium concentration Ag^+/45S5 Bioglass® scaffold and **d** high concentration Ag^+/45S5 Bioglass® scaffold

bioactive glass scaffold alone. They suggested that silver ion accumulation caused cell death and arrest of cell proliferation. Our results showed that higher concentration of silver incorporated into the scaffolds had reduced numbers of attached cells but no dead cells were observed after 1 week of culture.

4 Conclusions

45S5 Bioglass® based glass-ceramic scaffolds were fabricated by the foam replication technique, which produced scaffolds with a porosity of above 90%. The pore structure obtained fulfils the porosity requirement for bone TE in terms of pore size and interconnectivity, making these scaffolds highly suitable for their intended purpose in bone TE. The characterisation of these basic scaffolds, including bioactivity tests in SBF, showed that they conform to all previous work carried out on them. Thus these results gave confidence to the robustness of the fabrication technique and the reproducibility of the scaffold structure and properties. Silver was introduced into the chemical structure of the 45S5 Bioglass® based scaffolds through a molten salt ion exchange method. The characterisation tests showed that there is a saturation point where no more silver will be exchanged into the scaffold, with this occurring between 15 and 30 min of salt bath immersion. The porosity of the ion exchanged scaffolds was seen to decrease by the process however porosity did not fall below 65%. The ion exchange process led to an increase of the compressive strength of scaffolds, i.e. from 0.53 ± 0.08 MPa for plain 45S5 scaffolds up to $(0.62–0.73) \pm 0.04$ MPa for the ion exchanged samples before SBF immersion. After immersion in SBF the compressive strength of all the samples decreased. SBF immersion tests showed that the addition of silver into the composition of the scaffold has not affected the formation of HA on the scaffold surfaces, thus the scaffolds bioactivity is not impaired by the presence of Ag. The in vitro cell culture study indicated that the lower concentration of added silver ion supported cell attachment and maintained cell viability on 3D scaffolds comparable to the control (un-substituted) 45S5 Bioglass® scaffolds. Further biological studies are necessary to determine other possible cellular effects associated with the addition of silver ions to the scaffolds. Moreover the effect of silver ions on a bacterial cell suspension will be investigated to confirm the antimicrobial effect and to be able to draw a final conclusion on the optimal silver ion concentration to fulfil both purposes; of having the desired antimicrobial

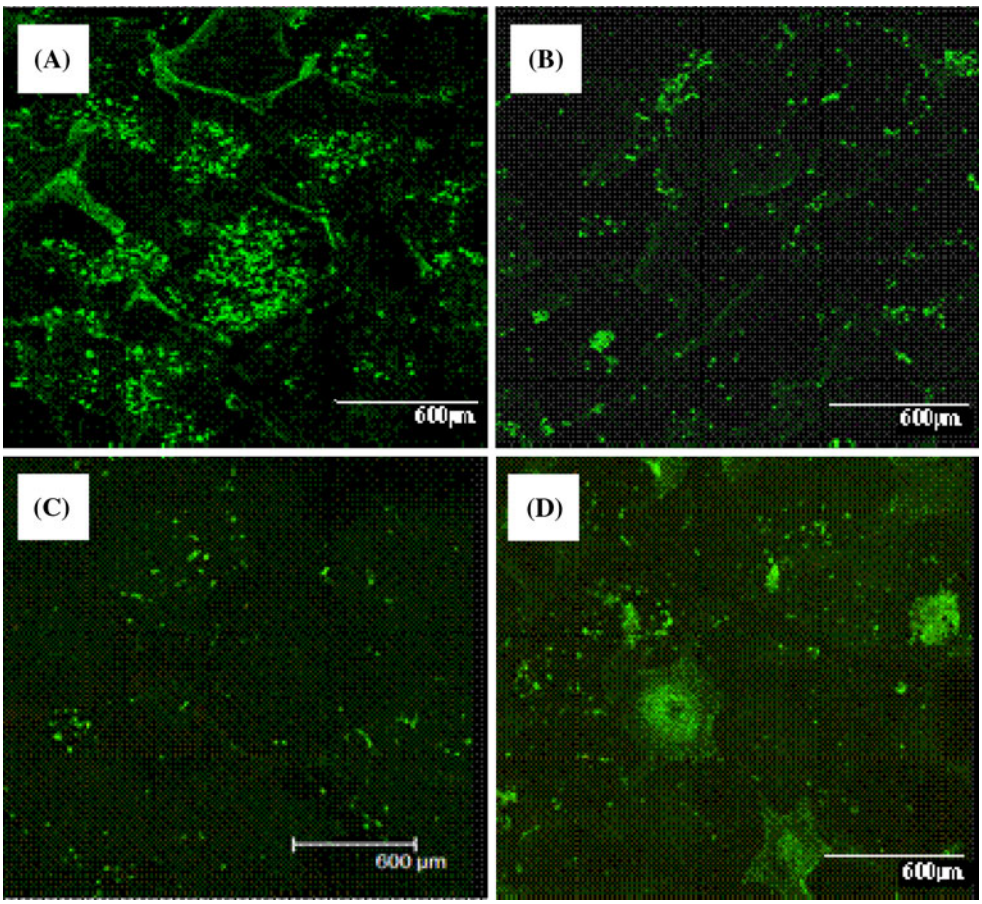

Fig. 12 HPDLCs attachment and viability on 3D Bioglass® scaffolds: **a** low concentration Ag^{+}/45S5 Bioglass® scaffolds, **b** medium concentration Ag^{+}/45S5 Bioglass® scaffolds, **c** High concentration Ag^{+}/45S5 Bioglass® scaffolds, and **d** plain 45S5 Bioglass® scaffold. Viable cells are stained green fluorescent with CMFDA (live marker). No dead cells (which would stain red with Ethidium homodimer-1) were observed

effect without jeopardizing bone cell viability, attachment and proliferation.

Acknowledgments The authors acknowledge financial support from EPSRC (UK).

References

1. Chen QZ, Thompson ID, Boccaccini AR. 45S5 Bioglass®-derived glass-ceramic scaffolds for bone tissue engineering. Biomaterials. 2006;27:2414–25.
2. Wu C, Ramaswamy Y, Boughton P, Zreiqat H. Improvement of mechanical and biological properties of porous CaSiO3 scaffolds by poly(D, L-lactic acid) modification. Acta Biomater. 2008;4:343–53.
3. Fu Q, Rahaman MN, Bal BS, Brown RF, Day DE. Mechanical and in vitro performance of 13–93 bioactive glass scaffolds prepared by a polymer foam replication technique. Acta Biomater. 2008;4:1854–964.
4. Hutmacher DW, Schantz JT, Lam CXF, Tan KC, Lim TC. State of the art and future directions of scaffold-based bone engineering from a biomaterials perspective. J Tissue Eng Regen Med. 2007;1:245–60.
5. Bucheler M, Haisch A. Tissue engineering in otorhinolaryngology. DNA Cell Biol. 2003;22:549–64.
6. Vitale-Brovarone C, Miola M, Balagna C, Verné E. 3D-glass-ceramic scaffolds with antibacterial properties for bone grafting. Chem Eng J. 2008;137:129–36.
7. Chen W, Liu Y, Courtney HS, Bettenga M, Agrawal CM, Bumgardner JD, Ong JL. In vitro anti-bacterial and biological properties of magnetron co-souttered silver-containing hydroxyapatite coating. Biomaterials. 2006;27:5512–7.
8. Di Nunzio S, Vitale Brovarone C, Spriano S, Milanese D, Verne E, Bergo V, Maina G, Spinelli P. Silver containing bioactive glasses prepared by molten salt ion exchange. J Eur Ceram Soc. 2004;24:2935–42.
9. Balagna C, Vitale Brovarone C, Miola M, Verne E, Canuto R A, Saracino S, Muzio G, Fucale G, Maina G. (2010) Biocompatibility and antibacterial effect of silver doped 3d-glass-ceramic scaffolds for bone grafting. J Biomater Appl in press.
10. Mouriño V, Boccaccini AR. Bone tissue engineering therapeutics: controlled drug delivery in three-dimensional scaffolds. J R Soc Interface. 2010;7:209–27.
11. Mäkinen TJ, Veiranto M, Knuuti J, Jalava J, Törmälä P, Aro HT. Efficacy of bioabsorbable antibiotic containing bone screw in the prevention of biomaterial-related infection due to *Staphylococcus aureus*. Bone. 2005;36:2.

12. Schmitz FJ, Jones ME. Antibiotics for treatment of infections cause by MRSA and elimination of MRSA carriage. What are the choices? Int J Antimicrob Agents. 1997;9:1–19.
13. Joostena U, Joist A, Gosheger G, Liljenqvist U, Brandt B, Von Eiff C. Effectiveness of hydroxyapatite-vancomycin bone cement in the treatment of *Staphylococcus aureus* induced chronic osteomyelitis. Biomaterials. 2005;26:25–30.
14. Ruparelia JP, Chatterjee AK, Duttagupta SP, Mukherji S. Strain specificity in antimicrobial activity of silver and copper nanoparticles. Acta Biomater. 2008;4:707–16.
15. Klueh U, Wagner V, Kelly S, Johnson A, Bryers JD. Efficacy of silver-coated fabric to prevent bacterial colonization and subsequent device-based biofilm formation. J Biomed Mater Res. 2000;53:621–31.
16. Varma RS, Kothari DC, Tewari R. Nano-composite soda lime silicate glass prepared using silver ion exchange. J Non-Cryst Solids. 2009;355:1246–51.
17. Akkopru B, Durucan C. Preparation and microstructure of sol–gel derived silver-doped silica. J Sol-Gel Sci Technol. 2007;43: 227–36.
18. Bellantone M, Coleman NJ, Hench LL. Bacteriostatic action of a novel four-component bioactive glass. J Biomed Mater Res. 2000;51:484–90.
19. Ahmed I, Abou Neel EA, Valappil SP, Nazhat SN, Pickup DM, Carta D, Carroll DL, Newport RJ, Smith ME, Knowles JC. The structure and properties of silver-doped phosphate-based glasses. J Mater Sci. 2007;42:9827–35.
20. Oven R, Yin M, Davies PA. Characterisation of planar optical waveguides formed by copper–sodium, electric field assisted, ion exchange in glass. J Phys D Appl Phys. 2004;37:2207–15.
21. Chen QZ, Efthymiou A, Salih V, Boccaccini AR. Bioglass®-derived glass-ceramic scaffolds: study of cell proliferation and scaffold degradation in vitro. J Biomed Mater Res Part A. 2008;84A:1049–60.
22. Suryanarayana C, Grant Norton M. X-ray diffraction: a practical approach. New York: Plenum Press; 1998. p. 21–96.
23. Kokubo T. A/W glass-ceramic: processing and properties. In: Hench LL, Wilson J, editors. An introduction to bioceramics. Singapore: World Scientific; 1993. p. 125–37.
24. Hench LL. Bioceramics. J Am Ceram Soc 1998; 1705–1728.
25. Somerman MJ, Archer SY, Imm GR, Foster RA. A comparative study of human periodontal ligament cells and gingival fibroblasts in vitro. J Dent Res. 1988;67:66–70.
26. Clupper DC, Hench LL. Bioactive response of Ag-doped tape cast Bioglass® 45S5 following heat treatment. J Mater Sci Mater Med. 2001;12:917–21.
27. Gough JE, Notingher I, Hench LL. Osteoblast attachment and mineralized nodule formation on rough and smooth 45S5 bioactive glass monoliths. J Biomed Mater Res Part A. 2004; 68A:640–50.
28. Kim CS, Park EK, Kim SG. Silica–silver nano structure spheres prepared by spray pyrolysis of sol containing silver precursor. J Sol–gel Sci Technol. 2008;47:7–15.
29. Pereira MM, Hench LL. Mechanisms of hydroxyapatite formation on porous gel-silica substrates. J Sol–Gel Sci Technol. 1996;7:59–68.
30. Yano T, Azegami K, Shibata S, Yamane M. Chemical state of oxygen in Ag+/Na+ ion-exchanged sodium silicate glass. J Non-Cryst Solids. 1997;222:94–101.
31. Xing ZC, Chae WP, Baek JY, et al. In vitro assessment of antibacterial activity and cytocompatibility of silver-containing PHBV nanofibrous scaffolds for tissue engineering. Biomacromolecules. 2010;11:1248–53.